

# 4-Mercaptophenylboronic Acid SAMs on Gold: Comparison with SAMs Derived from Thiophenol, 4-Mercaptophenol, and 4-Mercaptobenzoic Acid

David Barriet, Chi Ming Yam, Olga E. Shmakova, Andrew C. Jamison, and T. Randall Lee\*

Department of Chemistry, University of Houston, 4800 Calhoun Road, Houston, Texas 77204-5003

Received March 15, 2007. In Final Form: May 18, 2007

We report the formation and characterization of self-assembled monolayers (SAMs) derived from the adsorption of 4-mercaptophenylboronic acid (MPBA) on gold. For comparison, SAMs derived from the adsorption of thiophenol (TP), 4-mercaptophenol (MP), and 4-mercaptobenzoic acid (MBA) were also examined. The structure and properties of the SAMs were evaluated by ellipsometry, contact-angle goniometry, polarization-modulation infrared reflection–absorption spectroscopy (PM-IRRAS), and X-ray photoelectron spectroscopy (XPS). Specifically, ellipsometry was used to assess the formation of monolayer films, and contact angle measurements were used to determine the surface hydrophilicity and homogeneity. Separately, PM-IRRAS was used to evaluate the molecular composition and orientation as well as the intermolecular hydrogen bonding within the SAMs. Finally, XPS was used to evaluate the film composition and surface coverage (i.e., packing density), which was observed to increase in the following order: TP < MP < MPBA < MBA. A rationalization for the observed packing differences is presented. The XPS data indicate further that ultrahigh vacuum conditions induce the partial dehydration of MPBA SAMs with the concomitant formation of surface boronic anhydride species. Overall, the analytical data collectively show that the MPBA moieties in the SAMs exist in the acid form rather than the anhydride form under ambient laboratory conditions. Furthermore, stability studies find that MPBA SAMs are surprisingly labile in basic solution, where the terminal B–C bonds are cleaved by the attack of hydroxide ion and strongly basic amine nucleophiles. The unanticipated lability observed here should be considered by those wishing to use MPBA moieties in carbohydrate-sensing applications.

## Introduction

Thin-film technologies are increasingly used to study important biological processes, such as the recognition of proteins, lipids, and sugars on cell surfaces.<sup>1–6</sup> Both Langmuir–Blodgett films<sup>7</sup> and self-assembled monolayers<sup>8,9</sup> (SAMs) derived from the adsorption of alkanethiols, disulfides, and di-*n*-alkyl sulfides on gold have been extensively employed as mimics of cell membranes. The latter films have received considerable focus because of their well-defined structures, enhanced stabilities, and ease of formation and characterization.<sup>10</sup>

Sugars are involved at several levels in the metabolism of living organisms: they serve as structural building components and energy sources (glucose phosphates) and participate in a variety of physicochemical and biological processes.<sup>11</sup> In addition, carbohydrates represent a key component in the food industry.<sup>12</sup> Hydrogen-bonding interactions are currently the most important strategy employed to sense carbohydrates, either with designed

molecular receptors or with enzymes.<sup>13</sup> Most commonly used enzymatic sensors, however, suffer from two major drawbacks: (1) they are relatively unstable (thus limiting their use in industrial settings) and (2) only a few enzyme-based sensors are available (thus limiting the number of carbohydrates that can be sensed). Separately, the efficiency of molecular sensors based on hydrogen bonding is greatly reduced in aqueous media because water disrupts hydrogen-bonding networks and thus often prohibits *in vivo* sensing.

Compounds possessing the boronic acid group have shown both a strong affinity and a noticeable specificity to sugars.<sup>14</sup> Boronic acid can bind to 1,2- and 1,3-diols to form cyclic boronate esters via two separate mechanisms (depending on the solvent).<sup>15</sup> To understand these mechanisms and, in particular, to reveal the pathways involved in the recognition of sugars on cell surfaces, several model systems have been introduced that utilize compounds possessing boronic acid groups.<sup>14,16–18</sup> These systems rely on the strong affinity between boronic acids and sugars (both mono- and disaccharides).<sup>19</sup> A few self-assembled monolayers composed of both aliphatic<sup>20,21</sup> and aromatic<sup>22,23</sup> boronic acids as the sugar-recognition moiety have appeared in the

\* To whom correspondence should be addressed. E-mail: trlee@uh.edu.

(1) Pale-Grosdemange, C.; Simon, E. S.; Prime, K. L.; Whitesides, G. M. *J. Am. Chem. Soc.* **1991**, *113*, 12.

(2) Prime, K. L.; Whitesides, G. M. *Science* **1991**, *252*, 1164.

(3) Fischer, B.; Heyn, S. P.; Egger, M.; Gaub, H. E. *Langmuir* **1993**, *9*, 136.

(4) Kitano, H.; Ohno, K. *Langmuir* **1994**, *10*, 4131.

(5) Maeda, Y.; Yamamoto, H.; Kitano, H. *J. Phys. Chem.* **1995**, *99*, 4837.

(6) Yoshizumi, A.; Kanayama, N.; Maehara, Y.; Ide, M.; Kitano, H. *Langmuir* **1999**, *15*, 482.

(7) Nagahori, N.; Niikura, K.; Sadamoto, R.; Taniguchi, M.; Yamagishi, A.; Monde, K.; Nishimura, S.-I. *Adv. Synth. Catal.* **2003**, *345*, 729.

(8) Spinke, J.; Liley, M.; Guder, H.-J.; Angermaier, L.; Knoll, W. *Langmuir* **1993**, *9*, 1821.

(9) Gorman, C. B.; Miller, R. L.; Chen, K.-Y.; Bishop, A. R.; Haasch, R. T.; Nuzzo, R. G. *Langmuir* **1998**, *14*, 3312.

(10) Ulman, A. *Chem. Rev.* **1996**, *96*, 1533.

(11) Eggens, I.; Fenderson, B.; Toyokuni, T.; Dean, B.; Stroud, M.; Hakomori, S. *J. Biol. Chem.* **1989**, *264*, 9476.

(12) Barker, B. A. *Chem. Ber.* **1990**, *26*, 665.

(13) Barker, S. A. *Special Publication - R.S.C.* **1986**, *63*, 137.

(14) Narasimhan, K.; Wingard, L. B., Jr. *Anal. Chem.* **1986**, *58*, 2984.

(15) James, T. D.; Sandanayake Samankumara, K. R. A.; Shinkai, S. *Angew. Chem., Int. Ed.* **1996**, *35*, 1911.

(16) Kataoka, K.; Miyazaki, H.; Okano, T.; Sakurai, Y. *Macromolecules* **1994**, *27*, 1061.

(17) Hamachi, I.; Tajiri, Y.; Shinkai, S. *J. Am. Chem. Soc.* **1994**, *116*, 7437.

(18) Arimori, S.; Takeuchi, M.; Shinkai, S. *J. Am. Chem. Soc.* **1996**, *118*, 245.

(19) Lorand, J. P.; Edwards, J. O. *J. Org. Chem.* **1959**, *24*, 769.

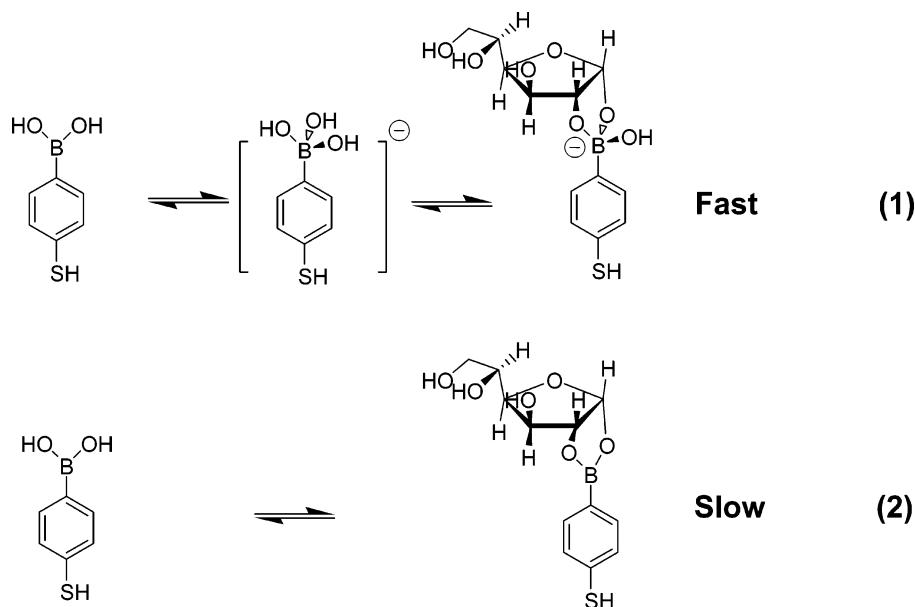
(20) Carey, R. I.; Folkers, J. P.; Whitesides, G. M. *Langmuir* **1994**, *10*, 2228.

(21) Weisbecker, C. S.; Merritt, M. V.; Whitesides, G. M. *Langmuir* **1996**, *12*, 3763.

(22) Kitano, H.; Kuwayama, M.; Kanayama, N.; Ohno, K. *Langmuir* **1998**, *14*, 165.

(23) Kanayama, N.; Kitano, H. *Langmuir* **2000**, *16*, 577.

## Scheme 1. Formation of the Boronate Esters in (1) Aqueous Media and (2) Aprotic Media



literature. However, most of the studies focused on the sensing capabilities of the system studied, dealing only briefly with the nature and packing structure of the adsorbates,<sup>22,23</sup> thereby limiting the conclusions that were drawn.

To transpose the chemistry of boronic acids from solution to self-assembled monolayers, several issues must be considered. In aqueous solution, only anionic boronates are formed (as long as the solution is sufficiently dilute).<sup>15</sup> Kinetics studies of the reaction between 1,2-diols and boronic acids have demonstrated that the formation of tetrahedral boronate intermediates is several orders of magnitude faster than the formation of trigonal boronates (Scheme 1).<sup>24</sup> On surfaces, however, the formation of a tetrahedral intermediate is disfavored sterically and electrostatically (assuming a negatively charged boronate species). Furthermore, electrostatic repulsion in SAMs has been observed for carboxylate-terminated films, giving rise to elevated  $pK_a$ 's for surface-bound acids when compared to those of their unbound analogs.<sup>25,26</sup> Similar effects might be anticipated for SAMs terminated with boronic acid groups. As such, the density of packing of the boronic acids might influence their binding with sugars through the steric repulsion of analytes or by creating unique binding geometries. In addition, the formation of intermolecular boronic anhydrides at the interface would remove some fraction of the tetrahedral anion from the acid–base equilibrium, changing the effective  $pK_a$  of boronic acid-terminated SAMs. The pH range in which sugars can bind to the boronic acid moiety (or “working pH” of the sensor) will also affect the nature of the analyte, owing to pyranose–furanose isomerization.<sup>15</sup> Consequently, this isomerization can also influence the binding efficiency because rigid vicinal cis diols are more prone to form stable boronate esters than other alcohols or diols.<sup>27</sup>

In an aprotic medium, the parameters needed to form a boronate ester would be either to reflux the boronic acid with the appropriate diol or to stir the two components together at room temperature in the presence of a dehydrating agent.<sup>20</sup> Furthermore, as long

as water is strictly excluded from the system, most boronic acids dehydrate to form stable boroxine trimers either when heated or under vacuum. These drawbacks, when combined with the questionable relevance of nonaqueous media in sugar sensing, renders this approach unattractive.

To circumvent these concerns and enhance our understanding of the interactions between sugars and boronic acid moieties anchored on a solid support, we report herein the preparation and characterization of SAMs derived from the simplest aromatic adsorbate, 4-mercaptophenylboronic acid (MPBA). The choice of this adsorbate was specifically motivated by several considerations. First, its relative structural simplicity when compared with the previously investigated systems<sup>22,23</sup> allows for an in-depth characterization. Second, the reactivities of aromatic boronic acids, due to their role in synthetic organic chemistry (Suzuki coupling),<sup>28</sup> are better understood than those of their aliphatic counterparts. Third, aliphatic boronic acids are sensitive to oxidation by atmospheric oxygen in a dry environment.<sup>29</sup> To complement our understanding of the MPBA system, we also prepared and characterized SAMs derived from the adsorption of structurally related thiophenol (TP), 4-mercaptophenol (MP), and 4-mercaptobenzoic acid (MBA). The structures of all adsorbates are shown in Figure 1. A variety of complementary surface analytical techniques were used to characterize the SAMs: ellipsometry, contact-angle measurements, polarization-modulation infrared reflection–absorption spectroscopy (PM-IRRAS), and X-ray photoelectron spectroscopy (XPS).

The high affinity of aromatic boronic acids for carbohydrates has been used previously to detect saccharides through absorption spectroscopy,<sup>30</sup> CD spectroscopy,<sup>31</sup> fluorescence spectroscopy,<sup>32</sup>

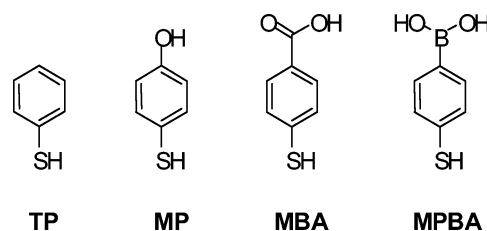


**Figure 1.** Structure of the adsorbates examined in this study, where TP = thiophenol, MP = *p*-mercaptophenol, MBA = *p*-mercaptobenzoic acid, and MPBA = *p*-mercaptophenylboronic acid.

(24) Wulf, G.; Dederichs, W.; Grostollen, R.; Jüpe, C. In *Affinity Chromatography and Related Techniques*; Gribnau, T. C. J., Visser, J., Nivard, J. F., Eds.; Elsevier: Amsterdam, 1982; p 207.

(25) Bain, C. D.; Whitesides, G. M. *Langmuir* **1989**, *5*, 1370.

(26) Lee, T. R.; Carey, R. I.; Biebuyck, H. A.; Whitesides, G. M. *Langmuir* **1994**, *10*, 741.

(27) Yan, J.; Springsteen, G.; Deeter, S.; Wang, B. *Tetrahedron* **2004**, *60*, 11205.

and electrochemistry.<sup>33</sup> For our purposes, we wish to use the present system (on flat gold and on gold nanoparticles) to sense carbohydrates using surface-enhanced Raman spectroscopy (SERS).<sup>34</sup> This technique relies on the enhancement of the Raman signal of a molecule when exposed to an electromagnetic field close to the interface of a noble metal (although most effective on silver surfaces, gold can also be used).<sup>35,36</sup> The strongest signal enhancement occurs when the distance between the metal interface and the recognition site is small.<sup>34</sup> To exploit this property and allow for a quantitative measurement of the analyte, we chose to use the relatively small MPBA molecule as the recognition moiety. Furthermore, we chose to avoid short-chain  $\omega$ -mercaptop aliphatic boronic acids because SAMs generated from short alkanethiols are disordered and sensitive to contamination.<sup>37</sup> Finally, the use of an aromatic ring allows for further functionalization in the ortho position; in particular, an amine group adjacent to the boronic acid can enhance the formation of stable boronate esters at physiological pH.<sup>38</sup>

### Experimental Section

**Materials.** Thiophenol (TP), 4-mercaptophenol (MP), and 4-mercaptobenzoic acid (MBA) were purchased from Aldrich and used without further purification. 4-Mercaptophenylboronic acid (MPBA) was either synthesized according to the published procedure<sup>39</sup> or purchased from Aldrich. Absolute ethanol and the contacting liquids were of the highest purity available and used as purchased.

**Substrate Preparation.** Substrates were prepared by the thermal evaporation of 1000 Å of gold onto silicon wafers Si(111), precoated with an adhesion layer of chromium (100 Å). The deposition was carried out at a rate of 1 Å/s under ultrahigh vacuum conditions. The resulting gold-coated wafers were rinsed with absolute ethanol and blown dry with ultrahigh purity nitrogen prior to adsorption of the thiols.

**SAM Preparation.** Ethanolic solutions of TP, MP, MBA, and MPBA, each at 1 mM concentration, were prepared in glass vials, which were previously cleaned with piranha solution (3:1 H<sub>2</sub>SO<sub>4</sub>/H<sub>2</sub>O<sub>2</sub>). (**Caution!** Piranha solution can react violently with organic compounds and should be handled with care.) The clean gold-coated wafers were immersed in the thiol solutions for 24 h, after which they were rinsed with absolute ethanol and blown dry with ultrahigh purity nitrogen before characterization.

**Ellipsometry.** A Rudolph Research Auto EL III ellipsometer operating with a 632.8 nm He–Ne laser at an angle of incidence of 70° from the surface normal was employed to measure the thickness of the SAMs. A refractive index of 1.45 was assumed for all films. The reported values represent the average of at least four measurements taken at different locations on the sample surface and were reproducible to within  $\pm 2$  Å of the value reported.

**Contact-Angle Measurements.** Contacting liquids were dispensed onto the surface of the SAMs using a Matrix Technologies micro-Electrapette 25. Advancing and receding contact angles were measured with a Ramé–Hart model 100 goniometer with the pipet

tip in contact with the drop. On average, 4 drops of contacting liquids were measured on different areas of the slide for each sample. The mean values were reproducible to within  $\pm 2^\circ$  of the value reported.

**Polarization-Modulation Infrared Reflection–Absorption Spectroscopy (PM-IRRAS).** A Nicolet Magna-IR 860 Fourier-transform spectrometer equipped with a liquid-nitrogen-cooled mercury–cadmium–telluride (MCT) detector and a Hinds Instruments PEM-90 photoelastic modulator (37 Hz) was employed to acquire the PM-IRRAS spectra. The data were collected at a spectral resolution of 4 cm<sup>-1</sup> for 256 scans using *p*-polarized light reflected from the sample at an angle of incidence of 80° from the surface normal.

**X-ray Photoelectron Spectroscopy (XPS).** A PHI 5700 X-ray photoelectron spectrometer equipped with a monochromatic Al K $\alpha$  X-ray source ( $h\nu = 1486.7$  eV) incident at 90° relative to the axis of a hemispherical energy analyzer was employed to collect the X-ray photoelectron spectra of the SAMs at a photoelectron takeoff angle of 45° from the surface and a pass energy of 23.5 eV. The binding energy scales were referenced to the Au 4f<sub>7/2</sub> peak at 84.0 eV. The XPS spectra were curve fitted, and the intensities (measured as peak areas) were calculated using Phi Multipak V 5.0A from Physical Electronics.

### Results and Discussion

**Ellipsometric Thicknesses.** Ellipsometry is commonly used to evaluate the quality of SAMs.<sup>40</sup> However, because the measured ellipsometric thicknesses can be strongly influenced by the quality of the underlying gold, one must assess this effect to obtain meaningful data. It is therefore judicious to consider the ellipsometric data for a new SAM with respect to that of known SAMs. The ellipsometric thicknesses of the SAMs generated for this investigation are  $\sim 4$  Å for TP,  $\sim 6$  Å for MP,  $\sim 9$  Å for MBA, and  $\sim 8$  Å for MPBA.<sup>41–45</sup> The first conclusion that we can draw from these average thicknesses for the SAM series is that they are all consistent with the formation of monolayer rather than multilayer films. Previous ellipsometric thicknesses reported for thiophenol monolayers on gold vary from about 1 to 5 Å;<sup>41–43</sup> this variation can be rationalized on the basis of varying substrate quality and experimental error, which is typically enhanced for extremely thin films.<sup>44,45</sup> Overall, the data suggest that TP and MP give rise to films that are poorly ordered and/or highly sensitive to experimental conditions.

The observed trend in thicknesses (TP < MP < MPBA < MBA) likely arises in part from two effects (1) differences in monolayer thickness based on adsorbate size (calculated as 7 Å for TP, 8 Å for MP, and 9 Å for both MPBA and MBA, assuming that the molecules are fully extended and oriented perpendicular to the surface)<sup>46</sup> and/or (2) differences in the surface coverage and tilt angle of the adsorbates. Furthermore, the measured thicknesses of the functionalized SAMs might be influenced by a possible ordering (or cooperativity) due to the presence of the para substituent. Specifically, the tail groups can interact favorably through dipole–dipole interactions, hydrogen bonding, and/or covalent cross linking. In addition, the electronic effects due to the tail groups might influence the degree of  $\pi$  stacking between

(28) Suzuki, A. In *Handbook of Organopalladium Chemistry for Organic Synthesis*; Negishi, E., Ed.; Wiley: Hoboken, NJ, 2002; p 249.

(29) Snyder, H. R.; Kuck, J. A.; Johnson, J. R. *J. Am. Chem. Soc.* **1938**, *60*, 105.

(30) Sandanayake, K. R. A. S.; Shinkai, S. *J. Chem. Soc., Chem. Commun.* **1994**, 1083.

(31) Shiomi, Y.; Kondo, K.; Saisho, M.; Harada, T.; Tsukagoshi, K.; Shinkai, S. *Supramol. Chem.* **1993**, *2*, 11.

(32) Metzger, A.; Lynch, V. M.; Anslyn, E. V. *Angew. Chem., Int. Ed. Engl.* **1997**, *36*, 862.

(33) Schuhmann, W.; Schmidt, H.-L. *Adv. Biosens.* **1992**, *2*, 79.

(34) Shafer-Peltier, K. E.; Haynes, C. L.; Glucksberg, M. R.; Van Duyne, R. P. *J. Am. Chem. Soc.* **2003**, *125*, 588.

(35) Haynes, C. L.; Van Duyne, R. P. *J. Phys. Chem. B* **2001**, *105*, 5599.

(36) Halteen, J. C.; Van Duyne, R. P. *J. Vac. Sci. Technol., A* **1995**, *13*, 1553.

(37) Bensebaa, F.; Ellis, T. H.; Badia, A.; Lennox, R. B. *Langmuir* **1998**, *14*, 2361.

(38) Lavigne, J. J.; Anslyn, E. V. *Angew. Chem., Int. Ed.* **1999**, *38*, 3666.

(39) Brikk, A.; Morin, C. *J. Organomet. Chem.* **1999**, *581*, 82.

(40) Ulman, A. *An Introduction to Ultrathin Organic Films: From Langmuir-Blodgett to Self-Assembly*; Academic Press: Boston, 1991.

(41) Whelan, C. M.; Barnes, C. J.; Walker, C. G. H.; Brown, N. M. D. *Surf. Sci.* **1999**, *425*, 195.

(42) Sabatani, E.; Cohen-Boulakia, J.; Bruening, M.; Rubinstein, I. *Langmuir* **1993**, *9*, 2974.

(43) Dhirani, A.-A.; Zehner, R. W.; Hsung, R. P.; Guyot-Sionnest, P.; Sita, L. R. *J. Am. Chem. Soc.* **1996**, *118*, 3319.

(44) Ulman, A. *Acc. Chem. Res.* **2001**, *34*, 855.

(45) Kang, J. F.; Liao, S.; Jordan, R.; Ulman, A. *J. Am. Chem. Soc.* **1998**, *120*, 9662.

(46) Dean, L. A. *Lange's Handbook of Chemistry*; McGraw-Hill: New York, 1999.

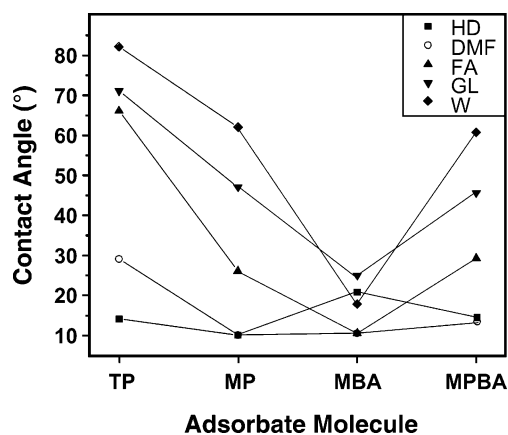


**Figure 2.** Advancing contact angles of hexadecane (HD), dimethylformamide (DMF), formamide (FA), glycerol (GL), and water (W) on the SAMs derived from thiophenol (TP), *p*-mercaptophenol (MP), *p*-mercaptobenzoic acid (MBA), and *p*-mercaptophenylboronic acid (MPBA).

the adsorbates.<sup>44</sup> Although unable to interact through hydrogen bonding because of steric constraints, the hydroxyl group in TP is, however, sufficiently polar to increase the electron density of the aromatic ring.<sup>47</sup> MBA can readily undergo intra-SAM hydrogen bonding,<sup>48</sup> possibly constraining the molecule to an upright orientation; the good agreement between the measured and calculated thicknesses supports this interpretation. Similarly, because of hydrogen bonding and/or cross linking (vide infra), the thickness of the film derived from MPBA is close to the predicted value.

**Contact Angle Measurements.** The wettability of surfaces functionalized with SAMs is highly dependent on the quality of the films and can be used as a probe of surface composition, structure, and coverage.<sup>40,49,50</sup> In particular, an initial evaluation of the contact angle hysteresis (i.e., the difference between the advancing and receding contact angles)<sup>51</sup> provides a rough indication of the degree of organization of the SAM, where more defects and/or poor packing in a monolayer will allow the contacting liquid to intercalate and reorganize the monolayer and thus will give rise to a change in the contact angle as the drop recedes across the surface.<sup>43</sup> Hysteresis values on the order of 10° are commonly recorded for SAMs derived from long-chain normal alkanethiols (i.e., ≥10 carbon atoms) and are associated with well-packed and well-ordered films stabilized by multiple interchain van der Waals interactions.<sup>52</sup> In contrast, SAMs derived from normal alkanethiols having short chains (i.e., ≤10 carbon atoms) are measurably higher.<sup>53</sup> Unfortunately, few reports are available in the literature regarding the wettability of small aromatic thiol-based monolayers on gold; furthermore, no hysteresis data are available.<sup>41–43</sup> The wettability data for our series, however, indicates that for all of the aromatic SAMs studied here the contact angle hysteresis for a variety of probe liquids is on the order of 20°, indicating imperfect order/packing for these SAMs (data not shown).

The value of the advancing contact angles provides additional information regarding SAM quality. Figure 2 shows the advancing contact angles of various types of contacting liquids on the aromatic SAMs: hexadecane (HD; apolar aprotic), dimethyl formamide (DMF; polar aprotic), and water, formamide, and glycerol (W, FA, and GL; polar protic). The HD contact angles indicate that all of the small aromatic thiols form high-energy surfaces, in contrast to the low-energy surfaces obtained from *n*-alkanethiols.<sup>40,50</sup> Previous studies of SAMs derived from TP on gold utilized water as the only contacting probe liquid, and the contact angles varied greatly from study to study.<sup>41–43</sup> In perhaps the most comprehensive investigation to date of aromatic thiols on gold,<sup>42</sup> Sabatini et al. reported that the contact angle of water on the SAM derived from TP was 80°, which is consistent with the value of 82° found here (Figure 2), leading us to conclude that our SAMs are of the highest quality currently possible (with regard to order and packing density) for self-assembled films of this type.

Our measured advancing contact angle of water (82°) on the SAM derived from TP is lower than that measured for well-ordered SAMs on gold derived from long-chain phenyl-terminated alkanethiols (92°).<sup>54</sup> This lower value might arise from enhanced attractive van der Waals forces between the water droplet and the underlying gold surface,<sup>55</sup> which for the present set of SAMs lies only a few angstroms beneath the interface. The low contact angle values might also be related to the orientation of the benzene ring. Indeed, Fox and Zisman<sup>56</sup> observed that the contact angles of various polar liquids were higher on single-crystal aromatics than on monolayers formed from the same aromatics; they concluded that the packing and thus the proportion of face-exposed aromatic rings were responsible for the observed differences in wettability. It is also possible that a low packing density in the present SAMs (vide infra) allows the contacting liquid to penetrate into the film and thereby give reduced contact angle values.

With the exception of hexadecane,<sup>57</sup> the contact angles of all probe liquids are highest for the SAMs derived from TP, intermediate for those derived from MP and MPBA, and lowest for those derived from MBA. These observations confirm the expected trend in surface hydrophilicity: TP < MP ≈ MPBA < MBA. The contact angles of water for MP, MBA, and MPBA are higher than anticipated when compared with the corresponding long-chain aliphatic thiols on gold: 63° for the MP SAM compared to <20° for  $\omega$ -mercaptoundecanol SAMs, 27° for the MBA SAM compared to <20° for  $\omega$ -mercaptohexadecanoic acid SAMs, and 61° for the MPBA SAM compared to ~20° for  $\omega$ -mercaptoundecylboronic acid SAMs.<sup>20,50</sup> This phenomenon is probably due to a combination of influences including, but not limited to, excessive contamination in the present SAMs, proximity to the underlying substrate, and/or interaction of the contacting liquids with the aromatic ring rather than the terminal group, an interpretation that assumes that the molecules are tilted.<sup>54</sup> Such a change in the tilt angle could arise from possible hydrogen bonding and/or covalent cross linking (vide infra).

**PM-IRRAS Studies.** PM-IRRAS is a sensitive technique that not only identifies the functionalities present at an interface but

(47) A comparison of the effective dipole moments of the adsorbates (TP = 1.2 D, MP = 1.5 D, MBA = 1.0 D, MPBA = 1.7 D) reveals that MPBA possesses the largest dipole. McClellan, A. L. *Tables of Experimental Dipole Moments*; Freeman: San Francisco, 1963.

(48) Wells, M.; Dermody, D. L.; Yang, H. C.; Kim, T.; Crooks, R. M. *Langmuir* **1996**, *12*, 1989.

(49) Allara, D. L.; Nuzzo, R. G. *Langmuir* **1985**, *1*, 45.

(50) Bain, C. D.; Troughton, E. B.; Tao, Y.-T.; Evall, J.; Whitesides, G. M.; Nuzzo, R. G. *J. Am. Chem. Soc.* **1989**, *111*, 321.

(51) de Gennes, P. G. *Rev. Mod. Phys.* **1985**, *57*, 827.

(52) Chaudhury, M. K. *Mater. Sci. Eng.* **1996**, *R16*, 97.

(53) Miura, Y. F.; Takenaga, M.; Koimo, T.; Graupe, M.; Garg, N.; Graham, R. L., Jr.; Lee, T. R. *Langmuir* **1998**, *14*, 5821.

(54) Lee, S.; Puck, A.; Graupe, M.; Colorado, R., Jr.; Shon, Y.-S.; Lee, T. R.; Perry, S. S. *Langmuir* **2001**, *17*, 7364.

(55) Miller, W. J.; Abbott, N. L. *Langmuir* **1997**, *13*, 7106.

(56) Fox, H. W.; Hare, E. F.; Zisman, W. A. *J. Colloid Sci.* **1953**, *8*, 194.

(57) The anomalously high contact angle for HD on the MBA SAM might arise from the enhanced adsorption of hydrocarbon-based contaminants on the surface of this SAM. The enhanced adsorption of contaminants is plausibly driven by the higher surface free energy of this SAM compared to that of the others. See, for example, Berg, J. C., Ed. *Wettability*; Marcel Dekker: New York, 1993.

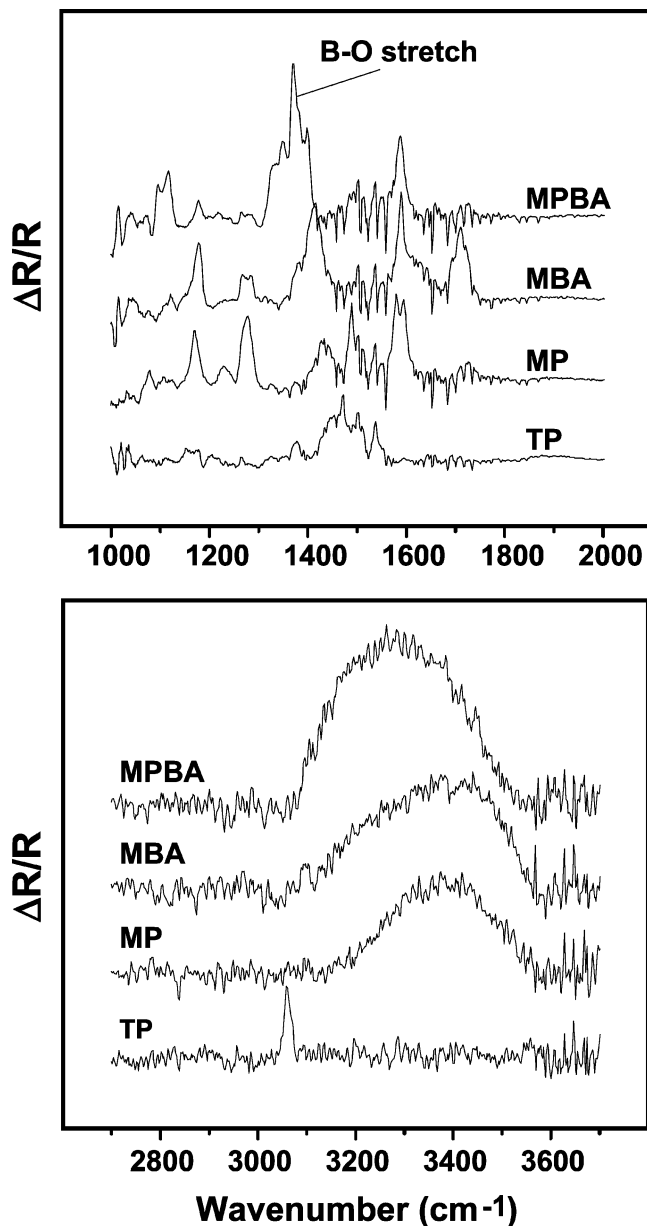


**Figure 3.** PM-IRRAS spectra for the SAMs derived from thiophenol (TP), *p*-mercaptophenol (MP), *p*-mercaptobenzoic acid (MBA), and *p*-mercaptophenylboronic acid (MPBA).

also probes slight variations in the surface structure of SAMs.<sup>37,58</sup> Figure 3 shows the PM-IRRAS spectra in the regions from 1000 to 2000  $\text{cm}^{-1}$  and 2800 to 3600  $\text{cm}^{-1}$  for the aromatic SAMs investigated here; Table 1 lists the major peak assignments. Aromatic C=C stretches in the region from  $\sim 1400$  to 1600  $\text{cm}^{-1}$  are common to all of the SAMs. Furthermore, all except the TP SAM exhibit band intensity in the region from  $\sim 1100$  to 1300  $\text{cm}^{-1}$ , indicating the presence of either C–O stretches (for MP and MBA) or a ring vibrational mode characteristic of boron-substituted aryls (for MPBA).<sup>59–61</sup> In the latter case, the weakness of this band is probably due to surface selection rules.<sup>62</sup> The broad bands above 3100  $\text{cm}^{-1}$  correspond to O–H stretches,

emerging either from the adsorbates or from water adsorbed at the interface of the substituted-aryl SAMs; unsurprisingly, these bands are absent in the SAM derived from TP. It is important to note here that XPS studies (vide infra) showed no hydrocarbon contamination for any of the aromatic SAMs. Taken as a whole, the PM-IRRAS data strongly support the presence of aromatic-based adsorbates on the surface of gold.

For the SAMs derived from TP, the anomalously low ellipsometric thickness and contact angle values when compared to those of the other aromatic SAMs (vide supra) might be interpreted to indicate that this adsorbate lies somewhat parallel to the surface.<sup>41</sup> The single band in the aromatic C–H stretching region at  $\sim 3070$   $\text{cm}^{-1}$ , however, appears to correspond to the C–H bond para to the sulfur atom. Support for this assignment is indicated by the absence of any corresponding C–H stretching band in the spectra of the other aromatic SAMs, where the adsorbates possess no C–H bond para to sulfur. As such, the presence of this band suggests some nontrivial degree of orientation along the surface normal for TP on gold.

For the SAMs derived from MP, we observed a strong band at 1280  $\text{cm}^{-1}$  characteristic of a phenol moiety (assigned to a combination of C–O stretches and O–H deformations) and a doublet at  $\sim 1600$   $\text{cm}^{-1}$  characteristic of the aromatic ring C=C stretch in a phenol.<sup>59</sup> No clear evidence of hydrogen bonding was found for the MP SAMs; in particular, the position of the band centered at 3400  $\text{cm}^{-1}$  might be due to water adsorbed on this high-energy surface.

For the SAMs derived from MBA, two major additional bands were observed: a broad one centered at  $\sim 1710$   $\text{cm}^{-1}$  (corresponding to the carbonyl group of a carboxylic acid) and a second band centered at  $\sim 1415$   $\text{cm}^{-1}$  (corresponding to the symmetric stretch of a carboxylate salt; as noted in the literature, the antisymmetric carboxylate stretch resonates at  $\sim 1590$   $\text{cm}^{-1}$ ).<sup>63–66</sup> We observed no distinct band at  $\sim 1740$   $\text{cm}^{-1}$  (characteristic of carboxylic dimers associated through double hydrogen bonding);<sup>63</sup> this result is consistent with recent reports noting the absence of this band for para-substituted MBA SAMs on gold.<sup>48</sup> Nevertheless, the absence of this band does not preclude the occurrence of less favored lateral hydrogen-bonding interactions between adjacent adsorbates.

For the SAMs derived from MPBA, the presence of the boronic acid moiety is indicated by the large and intense B–O stretching band centered at 1370  $\text{cm}^{-1}$ , which is consistent with that observed in the transmission IR spectra of MPBA in KBr glass.<sup>23,39,59</sup> Although the IR data allow us to confirm the presence of MPBA at the interface, our measurements cannot readily distinguish whether the boron-containing moieties exist as boronic acids or boronic anhydrides. According to the literature,<sup>67,68</sup> two separate bands can be used to determine the presence of anhydride: the disappearance of a band just above 1000  $\text{cm}^{-1}$  and the appearance of a new band around 700  $\text{cm}^{-1}$ . Unfortunately, PM-IRRAS suffers from a sharp decrease in sensitivity below 1000  $\text{cm}^{-1}$ ; consequently, we can use only the first criterion in our analysis.<sup>69</sup>

To this end, we performed three IR-based studies to assess the degree of anhydride formation (or covalent cross linking). First, we collected transmission IR spectra of phenyl boronic acid/

(63) Chidsey, C. E. D.; Loiacono, D. N. *Langmuir* **1990**, *6*, 682.

(64) Sun, L.; Kopley, L. J.; Crooks, R. M. *Langmuir* **1992**, *8*, 2101.

(65) Sun, L.; Crooks, R. M.; Ricco, A. J. *Langmuir* **1993**, *9*, 1775.

(66) Zhang, M.; Anderson, M. R. *Langmuir* **1994**, *10*, 2807.

(67) Snyder, H. R.; Konecky, M. S.; Lennarz, W. J. *J. Am. Chem. Soc.* **1958**, *80*, 3611.

(68) Santucci, L.; Gilman, H. *J. Am. Chem. Soc.* **1958**, *80*, 193.

(69) Even though we were able to observe a wide hydroxyl band over 3000  $\text{cm}^{-1}$ , this band could be due to water contamination on this high-energy surface rather than the hydroxyl group from the boronic acid.

(58) Wenzl, I.; Yam, C. M.; Barriet, D.; Lee, T. R. *Langmuir* **2003**, *19*, 10217.

(59) Socrates, G. *Infrared and Raman Characteristic Group Frequencies*; Wiley: New York, 2000.

(60) Nuzzo, R. G.; Dubois, L. H.; Allara, D. L. *J. Am. Chem. Soc.* **1990**, *112*, 558.

(61) Varsanyi, G. *Assignments for Vibrational Spectra of Seven Hundred Benzene Derivatives*; Wiley: New York, 1974.

(62) Bradshaw, A. M.; Richardson, N. V. *Pure Appl. Chem.* **1996**, *68*, 457.

Table 1. Peak Assignments for the Infrared Spectra of the Aromatic Thiols<sup>59–61,69</sup>

assignment	peak position (cm <sup>-1</sup> )			
	TP	MP	MBA	MPBA
C=O <sub>str</sub>			1709 (br, s)	
COO <sup>-</sup> <sub>asym str</sub>			1589 (s)	
aromatic C=C <sub>str</sub>	1471, 1571	1450–1650 (w) 1660 (doublet)	1450–1650 (w)	1450–1650 (w)
COO <sup>-</sup> <sub>sym str</sub>			1415	
B–O <sub>str</sub>				1370 (vs)
C–O <sub>str</sub>			1284	
C–OH <sub>str</sub> /O–H···O <sub>bend</sub>		1278 (br, vs)		
Ar–B ring mode				1270 (w)
C–H <sub>bend in plane</sub>	1170 (vw)	1170	1178	1178 (w) 1116 (s)

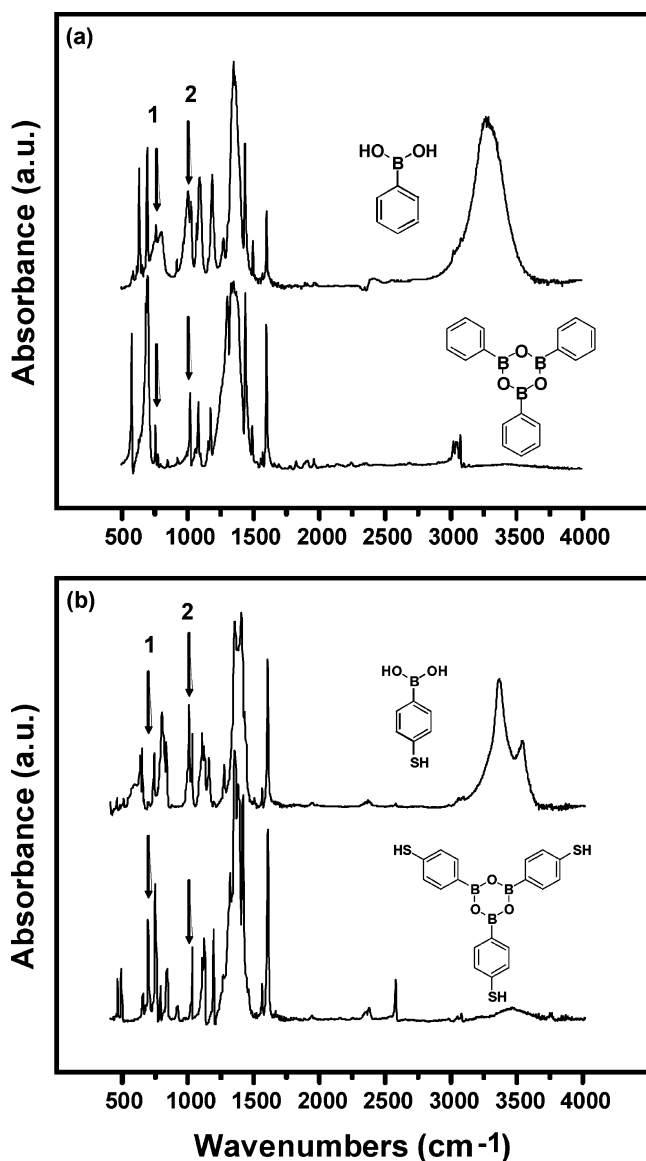


**Figure 4.** Transmission IR spectra for (a) phenyl boronic acid and anhydride and (b) mercaptophenyl boronic acid and anhydride. The bands marked 1 and 2 at  $\sim 700$  and  $\sim 1000$  cm<sup>-1</sup>, respectively, are characteristic of boronic acid/anhydride interchange.<sup>55</sup>

anhydride and mercaptophenyl boronic acid/anhydride to determine the position of the characteristic B–O bands (labeled 1 and 2, respectively, in Figure 4) as well as the position of any other bands at similar wavenumbers. Second, we compared the transmission IR spectra of both free molecules (Figure 4) to the PM-IRRAS spectrum of the MPBA SAM (Figure 3), which revealed that the broad band of medium intensity centered at

$\sim 1010$  cm<sup>-1</sup> in the transmission spectra is largely absent in the spectrum of the SAM. This loss of band intensity for the SAM might arise from a predominance of the anhydride form on the surface or from surface selection rules/orientational effects involving the acid form; unfortunately, we cannot distinguish these possibilities because no unambiguous assignment of the modes associated with these bands is available. Third, we attempted to form pure anhydride at the interface and analyze the structure by PM-IRRAS. Carey and co-workers<sup>20</sup> found that the formation of boronic anhydrides in aliphatic SAMs could be promoted through gentle warming or even simple immersion in a dry solvent. However, when we placed the MPBA SAM in dry isooctane or dry THF overnight or warmed it to 40 °C in dry isooctane for 1 h, we found no changes in the infrared spectrum. Whereas this result might be interpreted to indicate that the MPBA SAM exists in a predominantly anhydride form upon withdrawal from the ethanolic adsorbate solution, it is also possible that the SAM exists predominantly in the acid form and the formation of anhydride is rendered difficult in a 2D environment by the rigidity of the aromatic rings. Alternatively, the MPBA anhydride might be markedly less stable to atmospheric conditions than the anhydride studied by Carey et al.<sup>59,67</sup> Support for the latter interpretation (i.e., the predominance of the acid form under ambient conditions) is provided by data in a subsequent section (Structure as a Function of pH), where treatment of the MPBA SAM with acidic aqueous solution fails to influence the intensity of the weak band at  $\sim 1010$  cm<sup>-1</sup> (vide infra).

**XPS Studies.** X-ray photoelectron spectroscopy serves multiple purposes in the study of SAMs. The measured binding energies are sensitive to the electron density located on a specific atom and are primarily sensitive to the nature of the element considered and, secondarily, to the attached atoms. Therefore, XPS can be used to characterize SAMs both qualitatively and quantitatively.<sup>40</sup> Figure 5 shows XPS spectra of carbon (C 1s), oxygen (O 1s), sulfur (S 2p), and boron (B 1s) for the TP, MP, MBA, and MPBA SAMs; detailed assignments and precise peak positions are listed in Table 2. All spectra show the presence of carbon, oxygen, and sulfur with their expected binding energies.<sup>70</sup> In addition, the MPBA SAM exhibits a peak at  $\sim 191$  eV, which can be attributed to the boron atom in the SAM.<sup>48</sup>

In Figure 5a, the C 1s photoelectron peak centered at  $\sim 284$  eV with a shoulder at  $\sim 285$  eV in all spectra can be attributed to the carbon atoms of the aromatic ring and the electron-deficient carbon bonded to the electronegative sulfur atom, respectively.<sup>41</sup> Furthermore, the MBA SAM exhibits an additional C 1s peak at  $\sim 288$  eV, which can be attributed to the carbon atom in the carboxylate group.<sup>48</sup> As shown in Table 3, the cumulative C 1s photoelectron intensity increases in the following order: TP <

(70) Briggs, D.; Riviere, J. C. In *Practical Surface Analysis by Auger and X-ray Photoelectron Spectroscopy*; Briggs, D., Seah, M. P., Eds.; Wiley: Chichester, U.K., 1983; Chapter 3.

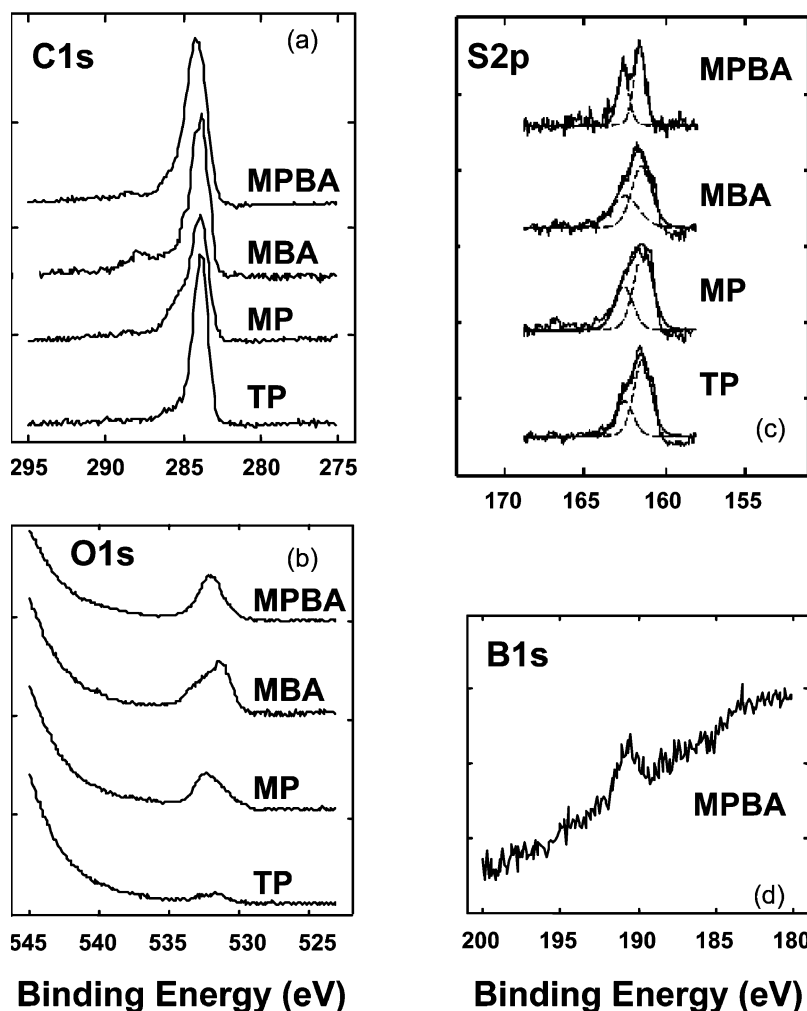


**Figure 5.** XPS spectra of C 1s, S 2p, O 1s, and B 1s regions of SAMs generated from thiophenol (TP), *p*-mercaptophenol (MP), *p*-mercaptobenzoic acid (MBA), and *p*-mercaptophenylboronic acid (MPBA).

**Table 2.** XPS Measurements of SAMs on Gold Generated from Thiophenol (TP), *p*-Mercaptophenol (MP), *p*-Mercaptobenzoic Acid (MBA), and *p*-Mercaptophenylboronic Acid (MPBA)<sup>a</sup>

element	binding energy (eV)			
	TP	MP	MBA	MPBA
C 1s	284.1, 286.0	284.0, 285.4	284.1, 285.5, 288.3	284.2, 285.8
O 1s	532.1 (weak)	532.1	531.2, 532.7	532.2
S 2p	162.0, 163.3	161.9, 162.3	162.1, 163.1	162.1, 163.3
B 1s			190.7	

<sup>a</sup> The values reported here are the average of three independent measurements. To compensate for sample charging, the binding energies were referenced to Au 4f<sub>7/2</sub> (84.0 eV).

MP < MPBA < MBA. When corrected for stoichiometry, the C 1s intensity for the MBA SAM is identical to that for the MPBA SAM. As a whole, the C 1s data suggests that the surface coverage (or packing density) increases as follows: TP < MP < MBA ≈ MPBA.

The peak at ~532 eV in Figure 5b demonstrates that all of the SAMs contain oxygen (Tables 2 and 3). The small quantity of oxygen found in the TP SAM probably arises from adventitious contaminants. Notably, the oxygen content of the MBA SAM is almost twice that of the SAMs derived from MP and MPBA, consistent with the stoichiometry of these molecules. For the MBA SAM, two distinct states for oxygen were observed, where the O 1s binding energies of 531.2 and 532.7 eV likely correspond to C=O and C–O oxygens, respectively.<sup>48</sup> For the MPBA SAM,

**Table 3.** Ratio of Signal Intensities of C 1s, O 1s, and S 2p to Au 4f<sub>7/2</sub> for Thiophenol (TP), *p*-Mercaptophenol (MP), *p*-Mercaptobenzoic Acid (MBA), and *p*-Mercaptophenylboronic Acid (MPBA)

	TP	MP	MBA	MPBA
XPS intensity ratio	0.054	0.066	0.081	0.071
C 1s/Au 4f <sub>7/2</sub>				
XPS intensity ratio	0.007	0.031	0.073	0.040
O 1s/Au 4f <sub>7/2</sub>				
XPS intensity ratio	0.013	0.016	0.020	0.018
S 2p/Au 4f <sub>7/2</sub>				
Au 4f <sub>7/2</sub> XPS intensity × 10 <sup>3</sup>	568	552	444	456

the observation of an O 1s photoelectron peak at 532.2 eV is consistent with that of boronic acid groups.<sup>20</sup>

Figure 5c shows photoelectron peaks with binding energies of ~162 and ~163.3 eV for all of the SAMs (Tables 2 and 3). These peaks can be assigned to the orbital doublet arising from S 2p<sub>3/2</sub> and S 2p<sub>1/2</sub>, respectively; the binding energies are consistent with sulfur bound to gold.<sup>70,71</sup> None of the SAMs exhibit a peak at 164 eV,<sup>72</sup> corresponding to unbound sulfur,<sup>70,71</sup> consequently,

(71) Laibinis, P. E.; Whitesides, G. M.; Allara, D. L.; Tao, Y.-T.; Parikh, A. N.; Nuzzo, R. G. *J. Am. Chem. Soc.* **1991**, *113*, 7152.

(72) Although the baseline in the spectrum of MPBA is unusually noisy at 165 eV, we note that other high-resolution XPS spectra of this SAM collected previously and not subjected to peak deconvolution showed zero intensity at this binding energy.

we can infer that all adsorbates bind to the surface of gold through the sulfur atoms. Upon deconvolution of the sulfur spin-orbit doublet, we found that the ratio between the low-energy ( $S\ 2p_{3/2}$ ) and high-energy ( $S\ 2p_{1/2}$ ) components of the sulfur doublet varied somewhat from sample to sample. Whereas the ratios for TP and MP were close to the theoretical value (2:1),<sup>20,73</sup> those for MBA and MPBA were noticeably smaller (1.4:1). Similar discrepancies have been reported in the literature<sup>74,75</sup> and are generally attributed to the presence of small amounts of disulfide species.

In Figure 5d, the B 1s photoelectron peak with binding energy of 190.7 eV is observed at lower binding energy than that observed for  $\omega$ -mercaptoalkylboronic acid (192 eV) and the published value for *p*-chlorobenzeneboronic acid (191.5 eV).<sup>20</sup> A lower binding energy corresponds to enhanced electron density localized on the boron atom. Given that the formation of a tetrahedral boronic anhydride gives rise to a net negative formal charge on boron, we propose that the observed low binding energy for the MPBA SAM arises from the (at least partial) formation of tetrahedral boron moieties in the monolayer.<sup>20,76</sup>

After correcting the raw intensities for the Scofield cross sections of ionization,<sup>70</sup> we obtained a ratio of O 1s/B 1s equal to 1.3,<sup>77</sup> consistent with the substantial dehydration of boronic acid with the formation of anhydride (perhaps occurring under vacuum during XPS analysis).<sup>78,79</sup> Otherwise, we would expect a ratio of oxygen to boron of 2.0 for free boronic acids. In their study of SAMs derived from  $\omega$ -mercaptoundecylboronic acid, Carey et al. obtained a ratio of boron to oxygen of 1.0.<sup>20</sup> We rationalize the difference between their ratio and our ratio by considering a long, flexible aliphatic chain with respect to a short, stiff aromatic ring, respectively. The structural features of the latter prevent the adsorbates from reorganizing efficiently; as a consequence, the degree of cross linking for the latter system is less than that for the more flexible aliphatic system. In addition,  $\pi$ - $\pi$  stacking interactions are generally stronger than van der Waals interactions;<sup>80</sup> as such,  $\pi$ - $\pi$  stacking optimization might partially restrict the formation of boronic anhydride cross links. Furthermore, the cross-linking process is highly favored in the case of the  $\omega$ -mercaptoundecylboronic acid SAMs because the gain in energy from dehydration is more important than the loss of energy that is consequent with a loss of crystallinity. Given these collective considerations, we propose that the oxygen-to-boron ratio of 1.3 is consistent with the surface prevalence of one or both of the structures shown in Figure 6 (or a superstructure based on these units).

Table 3 also shows the ratio of S 2p/Au 4f<sub>7/2</sub> for the SAMs, of which both sulfur and gold undergo similar attenuation due to direct attachment of the sulfur atoms to the gold substrate. Given this fact and the fact that all of the adsorbates contain a

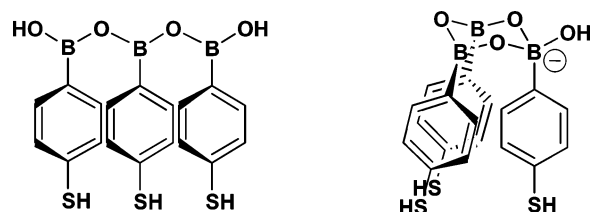


**Figure 6.** Possible surface configurations for SAMs derived from *p*-mercaptophenylboronic acid (MPBA).

single sulfur atom, the sulfur-to-gold ratio can be used to measure the packing density, which we interpret to increase in the following order: TP < MP < MPBA < MBA. The difference in packing density between the TP SAMs and the MP SAMs can plausibly arise from enhanced  $\pi$ - $\pi$  interactions due to the electron-donating ability of the OH group. We note that no evidence of hydrogen bonding was found within the MP monolayer, probably owing to the rigidity of the aromatic system.

Similarly, the intensity of the Au 4f<sub>7/2</sub> photoelectron signal for SAMs can be used to estimate the packing density of SAMs.<sup>81</sup> Table 3 shows that the Au 4f<sub>7/2</sub> intensities decrease in the following order: TP  $\approx$  MP > MBA  $\approx$  MPBA, indicating that the thinnest layers are generated from TP and MP and the thickest layers are generated from MBA and MPBA; these observations are consistent with the conclusions in the preceding paragraph and with the ellipsometric data (vide supra). The packing density of the SAMs appears to be strongly influenced by stabilizing  $\pi$ - $\pi$  interactions and/or tail-group interactions between the adsorbate molecules.

**Structure as a Function of pH.** To probe further the nature of the aromatic boronic acid/anhydride at the interface, we examined the properties of the SAM as a function of pH. Several investigations regarding the pH-dependent structure of *p*-mercaptophenylbenzoic acid SAMs were reproduced here to assess the validity/reproducibility of our methods.<sup>65</sup> Bain and co-workers<sup>25</sup> performed contact angle titrations on SAMs derived from  $\omega$ -mercaptohexadecanoic acid (MHDA) and observed a positive shift (+3) in pK<sub>a</sub> (or rather the midpoint in the titration) for the carboxylic acid on the surface compared with that in solution. This shift in equilibrium between carboxylic acid and carboxylate was justified by a change in the local dielectric environment of the group at the surface: as the degree of ionization increased, the electric field at the interface disfavored the additional formation of carboxylate, giving rise to the upward shift in pK<sub>a</sub>.<sup>26</sup> A shift of the same order of magnitude was also observed for amine-terminated SAMs as well as for SAMs generated from the adsorption of  $\omega$ -mercaptoundecylboronic acid.<sup>21</sup> Because boronic acids act more as Lewis acids and carboxylic acids act more as Brønsted acids, we investigated further their behavior at the interface. In addition, we examined whether the structure and/or distance between the functional group and the surface exerted any influence on the extent of ionization.

The ionization of SAMs derived from aliphatic MHDA and aromatic MBA was estimated qualitatively using the ratio of the band intensity of the carboxylic acid ( $\sim 1730\text{ cm}^{-1}$ ) and that of the carboxylate ( $\sim 1430\text{ cm}^{-1}$ ). Before analysis, all samples were left to equilibrate for 30 min in unbuffered solution of the indicated pH. (We note that no differences in the spectra were observed when new samples were analyzed at each pH.) Figure 7 shows that the carboxyl moieties in the MBA SAM behave similarly to those in the MHDA SAM; the similar behavior suggests that

(73) Frey, S.; Stadler, V.; Heister, K.; Eck, W.; Zharnikov, M.; Grunze, M.; Zeysing, B.; Terfort, A. *Langmuir* **2001**, *17*, 2408.

(74) Mekhalif, Z.; Riga, J.; Pireaux, J.-J.; Delhalle, J. *Langmuir* **1997**, *13*, 2285.

(75) Magnee, R.; Mekhalif, Z.; Doneux, C.; Duwez, A.-S.; Gregoire, C.; Riga, J.; Delhalle, J.; Pireaux, J. J. *J. Electron. Spectrosc.* **1998**, *88*-91, 855.

(76) Hendrickson, D. N.; Hollander, J. M.; Jolly, W. L. *Inorg. Chem.* **1970**, *9*, 612.

(77) To ensure of the validity of our boron-to-oxygen ratio, several tests were performed. First, the degree of oxygen contamination was carefully monitored using thiophenol as a reference. Second, the monolayer was formed using both anhydride and free acid, yielding no difference in the ratio. Third, the synthesized boronic acid and the purchased sample showed identical results.

(78) XPS cannot probe the concentration of elemental hydrogen. We note that the difference in electronegativity between hydrogen and boron (1.85 and 2.05 on the Pauling scale, respectively)<sup>79</sup> is insufficient to produce any shift in binding energy for O 1s between boronic and boroxine.

(79) March, J. *Advanced Organic Chemistry: Reactions, Mechanism, and Structure*, 3rd ed.; Wiley: New York, 1986.

(80) Jin, Q.; Rodriguez, J. A.; Li, C. Z.; Darici, Y.; Tao, N. J. *Surf. Sci.* **1999**, *425*, 101.

(81) Park, J.-S.; Vo, A. N.; Barriet, D.; Shon, Y.-S.; Lee, T. R. *Langmuir* **2005**, *21*, 2902.



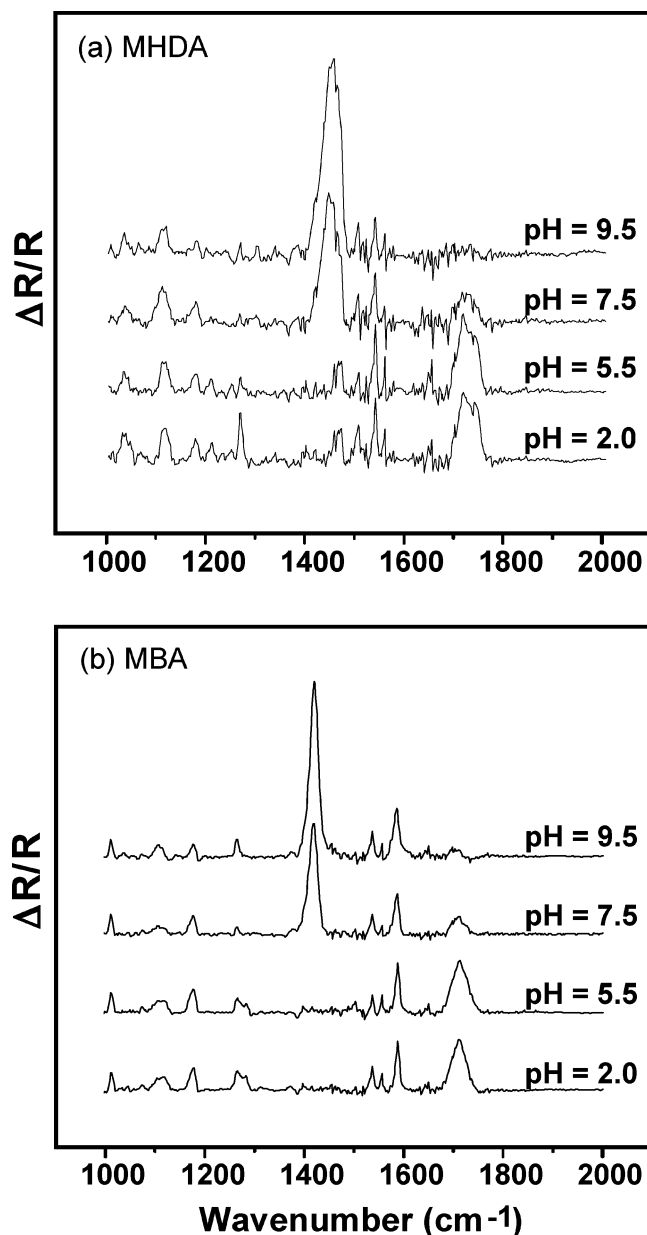


**Figure 7.** Evolution of the PM-IRRAS spectra of SAMs generated from (a)  $\omega$ -mercaptohexadecanoic acid and (b) *p*-mercaptobenzoic acid as a function of pH.

the underlying gold surface exerts no strong influence on the overall dielectric environment at the interface of the monolayer.

When submitted to the same treatment, the MPBA SAM behaved in a radically different manner than its carboxylic acid counterparts. We had contemplated using the B–O stretching band around  $1350\text{ cm}^{-1}$  as an indication of the degree of ionization of the boronic acid because it is known that this band is severely diminished upon completion of the octet of the boron (through the complexation of a third oxygen atom).<sup>82</sup> However, when exposed to the various pH environments, the MPBA SAMs appeared to behave erratically when compared with other known systems that express boronic acid moieties (aromatic or aliphatic) at interfaces (Figure 8).<sup>20,22</sup> In particular, we observed the greatest B–O band intensity for SAMs soaked in ethanol with no clear trend as one progresses from soaking the SAMs at pH's ranging from 2.0 to 9.5. The B–O band intensity was, however, sharply lowered after soaking at pH 9.5. Even though the stability of the boronic acid was not investigated per se in the report by Carey

(82) Letsinger, R. L.; Hamilton, S. B. *J. Am. Chem. Soc.* **1958**, *80*, 5411.

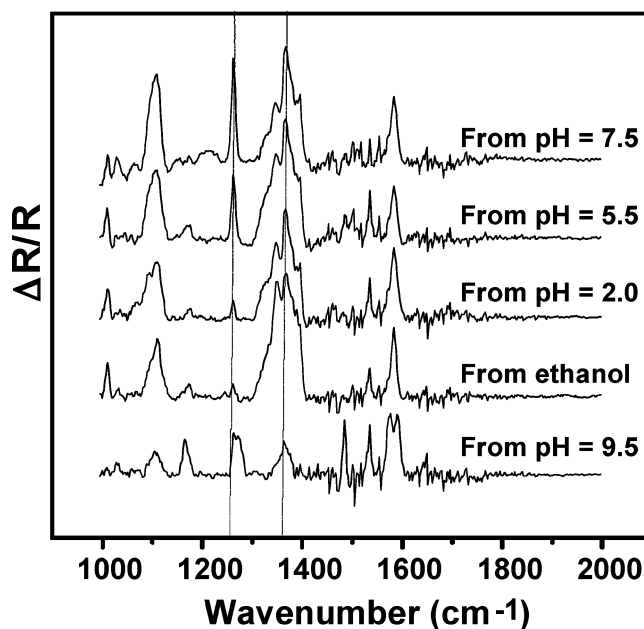


**Figure 8.** Evolution of the PM-IRRAS spectra of SAMs generated from *p*-mercaptophenylboronic acid (MPBA) as a function of pH. We have assigned the band at  $1267\text{ cm}^{-1}$ , whose intensity was observed to increase with the pH of the solution, to adventitious contaminants arising from the rinsing procedure.

et al.,<sup>20</sup> their ability to measure contact angles at high pH presumes the stability of this monolayer under highly basic conditions. In contrast, the analysis of the MPBA SAM by XPS showed that, rather than simple complexation by a hydroxide group, the diminishment of the B–O stretch at high pH is associated with a loss of boron from the monolayer (Figure 9). On the basis of absolute peak intensities, the loss of boron is accompanied by a partial loss of sulfur and carbon as well, although the loss of the latter species is minor when compared to the loss of boron. We note that the oxidation of boron to form metaborates is a known process leading to B–C bond cleavage.<sup>29,83</sup> Although the use of deoxygenated water had no effect on the experimental results, we cannot rule out the involvement of trace amounts of oxygen.

Importantly, Figure 8 also shows that the intensity of the boronic acid band<sup>67,68</sup> at  $\sim 1010\text{ cm}^{-1}$  is similar regardless of whether the SAM was previously exposed to ethanol or to water at pH 2.0 and 5.5 (aqueous conditions where the monolayer is presumably stable). Given the known facile hydrolysis of boronic anhydrides in water,<sup>84</sup> this observation strongly suggests that the MPBA SAM exists in the acid form rather than the anhydride form under ambient conditions (*vide supra*).

We performed a brief kinetics study at various pH's to examine the reactivity of boron in the MPBA SAMs. Using a combination of IR and XPS analyses, we found that whereas the MPBA SAMs appeared to be unaffected by a prolonged (over 4 h) immersion in water at neutral pH the content of boron in the monolayer progressively decreased at pH 9 and was almost entirely depleted after a few minutes at pH 12. These observations are consistent with a mechanism in which the complexation of boronic acid with a third hydroxyl group is followed by facile cleavage of the B–C bond, driving the system toward a boron-free monolayer. This peculiar behavior toward basic hydrolysis confirms that the reactivity of MPBA SAMs is distinct from that of both aromatic boronic acids in solution<sup>15</sup> and the aliphatic boronic acid SAM

(83) The use of deoxygenated water had no effect on the outcome of the hydrolysis. The presence of trace amounts of oxygen, however, cannot be ruled out.

(84) Please see reference 20 and references therein.

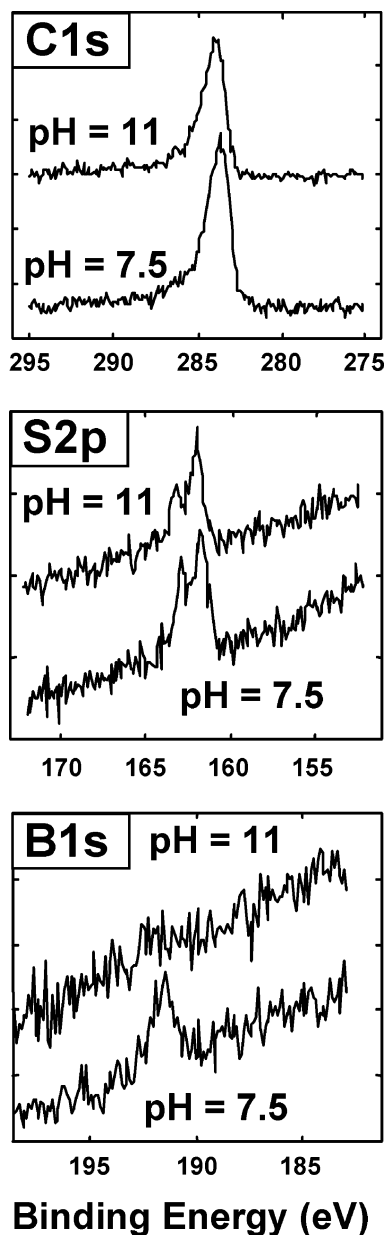


**Figure 9.** XPS spectra of the C 1s, S 2p, and B 1s regions of SAMs generated from *p*-mercaptophenylboronic acid (MPBA) at pH 7.5 and 11.

studied by Carey and co-workers.<sup>20</sup> It is possible that a structure similar to that suggested above by the XPS studies (Figure 6) is responsible for the enhanced sensitivity to base-promoted B–C bond cleavage in the MPBA SAM.

We further probed the base-sensitive nature of the MPBA SAM by examining the reactivity of the monolayer toward a variety of amines (i.e., dodecylamine, triethylamine, and pyridine). Upon immersing the monolayer in a solution of the corresponding amine at 1 mM concentration in dry pentane for 1 h, no B 1s signal was observed when dodecylamine was used as the nucleophile/base, only a small fraction was present for triethylamine, and no change was observed with pyridine (Figure 10). We rationalize these observations by considering the nucleophilic strength of the amines: both dodecylamine and triethylamine are strong Lewis bases that act as strong nucleophiles to attack the boron atom; however, pyridine fails to attack the monolayer because it is a weak Lewis base and a weak nucleophile. It is worth noting that the bulkiness of triethylamine probably slows the kinetics of the attack on boron, a conclusion drawn from the fact that a weak B 1s signal is still present after 1 h (Figure 10);

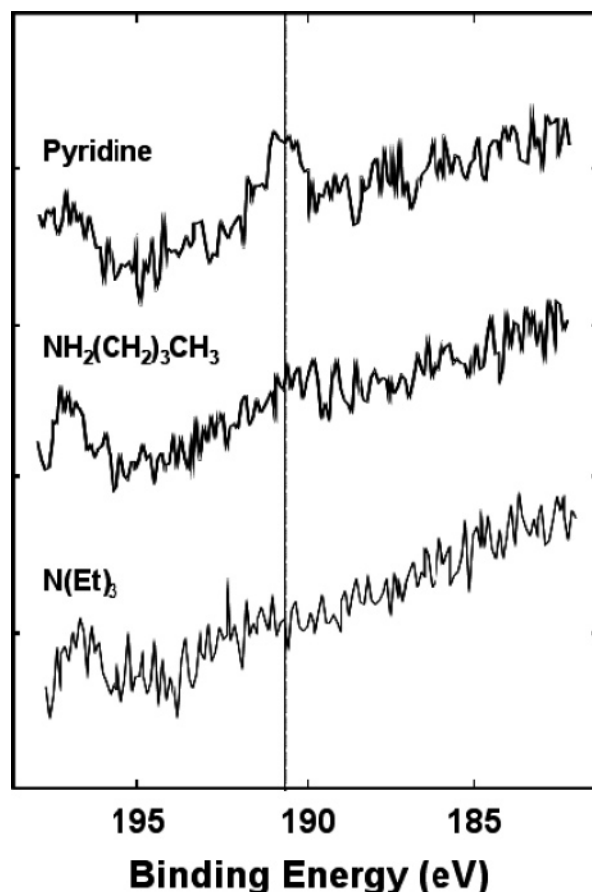


**Figure 10.** XPS spectra of the B 1s region of SAMs generated from *p*-mercaptophenylboronic acid (MPBA) treated with pyridine, tetradecylamine, and triethylamine for 1 h at 1 mM concentration in pentane.

consequently, it appears that the nucleophilic attack on boron is involved in the rate-determining step of the base-promoted degradation of MPBA SAMs.

## Conclusions

These studies demonstrate the formation of self-assembled monolayers from the adsorption of 4-mercaptophenylboronic acid (MPBA) on gold as demonstrated by the complementary surface characterization techniques of ellipsometry, contact-angle goniometry, PM-IRRAS, and XPS. The MPBA SAMs were compared to those derived from structurally related thiophenol (TP), 4-mercaptophenol (MP), and 4-mercaptobenzoic acid (MBA). The packing density (surface coverage) of the SAMs was observed to increase in the following order: TP < MP < MPBA < MBA. Analysis by PM-IRRAS revealed no definitive evidence of interchain hydrogen bonding in any of the SAMs; consequently, we attribute the observed differences in order/packing to differences in intermolecular  $\pi$  stacking and/or cross linking of the tail groups. Partial dehydration of the MPBA SAMs with consequent anhydride formation occurred upon analysis by XPS under ultrahigh vacuum. Importantly, studies of stability in solution revealed that the boron moiety in MBPA SAMs is sensitive to basic conditions, undergoing B–C bond cleavage at high pH and in the presence of strong amine nucleophiles.

**Acknowledgment.** We gratefully acknowledge financial support from the National Science Foundation (DMR-0447588) and the Robert A. Welch Foundation (E-1320).